Adsorption of Phenylphosphonic Acid on GaAs (100) Surfaces

A. M. Botelho do Rego,*,† A. M. Ferraria,† J. El Beghdadi,‡ F. Debontridder,‡ P. Brogueira,§ R. Naaman,⊥ and M. Rei Vilar‡

Centro de Química Física Molecular and ICEMS, Departamento de Física, Instituto Superior Técnico, P-1049-001 Lisboa, Portugal, ITODYS (CNRS - Université Denis Diderot), F-75005 Paris, France, and Chemical Physics Department, Weizmann Institute of Science, Rehovot, Israel 76100

Received March 14, 2005. In Final Form: June 15, 2005

The adsorption of phenylphosphonic acid (PPA) on GaAs (100) surfaces from solutions in acetonitrile/water mixtures was studied using Fourier transform infrared spectroscopy in attenuated total reflection in multiple internal reflections (ATR/MIR), X-ray photoelectron spectroscopy (XPS), high-resolution electron energy loss spectroscopy (HREELS), and atomic force microscopy (AFM). ATR/MIR in situ showed that the accumulation of PPA molecules near the GaAs surface increased with the water concentration in the solution. For water contents lower than 4%, ATR/MIR and XPS results are consistent with the formation of a low-density monolayer. A mechanism is proposed for H_2O percentages lower than 4% involving the creation of interfacial bonds through a Brønsted acid−base reaction, which involves the surface hydroxyl groups most probably bound to Ga. It was found that the morphology of the final layer depended strongly on the water concentration in the adsorbing solution. For water concentrations equal to or higher than 5%, the amount of adsorbed molecules drastically increased and was accompanied by modifications in the infrared spectral region corresponding to P−O and P═O. This sudden change indicates a deprotonation of the acid. XPS studies revealed the presence of extra oxygen atoms as well as gallium species in the layer, leading to the conclusion that phosphonate and hydrogenophosphonate ions are present in the PPA layer intercalated with H_3O^+ and Ga^{3+} ions. This mechanism enables the formation of layers ∼10 times thicker than those obtained with lower H_2O percentages. HREELS indicated that the surface is composed of regions covered by PPA layers and uncovered regions, but the uncovered regions disappeared for water contents equal to or higher than 5%. XPS results are interpreted using a model consisting of a monolayer partially covering the surface and a thick layer. This model is consistent with AFM images revealing roughness on the order of 7 nm for the thick layer and 0.2−0.5 nm for the thin layer. Sonication proves to be an effective method for reducing layer thickness.

Introduction

Semiconductor surface chemistry is currently a field of increasing interest because hybrid structures based on organic and inorganic semiconductor materials can be used for various technological applications, specifically as chemical sensors. The molecules are usually chemisorbed to couple molecular and semiconductor properties and to stabilize the semiconductor surfaces. Controlling the adsorption process and its characterization remains a challenge, especially in the case of III−V semiconductors, in which the surfaces are chemically unstable.[1] In fact, because of the high carrier mobility, gallium arsenide (GaAs) is a promising material for building fast-response electronic devices for chemical sensing.[2] Another interesting characteristic of GaAs is the ability to create heterojunctions that enable the confinement of carriers near the surface. The use of GaAs properties is the basis of the development of recent hybrid (organic−inorganic) systems, particularly sensors.[3] There, a molecular monolayer coating is deposited to selectively recognize the analyte. The study of the interfacial bond as well as the fractional coverage of the molecular adsorption to the surface is crucial. In this study, the reactivity of GaAs surfaces was tested by using a model molecule: phenylphosphonic acid (PPA).

The phosphonic function was used for molecular grafting on GaAs. In fact, phosphorus-based acids were found to have large affinity toward oxidized surfaces.[4,5] Infrared spectroscopy has shown that films are formed by the reaction of organic phosphonate with a steel surface that produces a metal salt. This reaction has been used, for instance, to create a corrosion protection on carbon steels.[6] Identical reactions were also employed on TiO_2 and WO_3 substrates[7] and used on sensors for toxic gases such as CO, NO_x, H_2S, and organic vapors. Strong bonding and high fractional coverage by phosphonates on both titanium and its alloys can also be obtained.[8] The binding of organic phosphate to GaAs was investigated as a possible way to

* Corresponding author: Ana Maria Botelho do Rego, Centro de Química-Física Molecular, Instituto Superior Técnico, P-1049−001 Lisboa Portugal; Tel.: 351 21 8419255; fax: 351 21 8464455; e-mail: amrego@ist.utl.pt.

† Centro de Química Física Molecular, Instituto Superior Técnico.

‡ CNRS - Université Denis Diderot.

§ Weizmann Institute of Science.

⊥ Departamento de Física, Instituto Superior Técnico.

(1) Seker, F.; Meeker, K.; Kuech, T.; Ellis, A. B. *Chem. Rev*. **2000**, *100*, 2505.

(2) Brodsky, M. H. *Sci. Am.* **1990**, *262* (2), 68.

(3) Ashkenasy, G.; Cahen, D.; Cohen, R.; Shanzer, A.; Vilan, A. *Acc. Chem. Res.* **2002**, *35*, 121.

(4) Guilbault G. G.; Scheide, E. P. *J. Inorg. Nucl. Chem.* **1970**, *32*, 2959.

(5) Nowack, B. *Water Res.* **2003**, *37*, 2533.

(6) To, X. H.; Pebere, N.; Pelabrat, N.; Boutevin, B.; Hervaud, Y. *Corros. Sci.* **1997**, *10−11*, 1925.

(7) Kim, C. S.; Lad, R. J.; Tripp, C. P. *Sens. Actuators, B* **2001**, *76*, 442.

(8) Schwartz, J.; Avaltroni, M. J.; Dnahy, M. P.; Silverman, B. M.; Hanson, E. L.; Schwarzbauer, J. E.; Midwood, K. S.; Gawalt, E. S. *Mater. Sci. Eng., C* **2003**, *23*, 395.

10.1021/la050682+ CCC: $30.25
Published on Web 08/10/2005

chemisorb organic molecules on GaAs surfaces to increase their biocompatibility; this bonding was found to be stronger than that of carboxylic groups, which, in turn, were stronger binders than thiols.[9]

In this work, we investigated the adsorption of PPA on etched GaAs (100) surfaces using surface analysis techniques to characterize the adsorbed layer. The techniques used for characterizing the adsorption process are attenuated total reflection in multiple internal reflections (ATR/MIR), X-ray photoelectron spectroscopy (XPS), high-resolution electron energy loss spectroscopy (HREELS), and atomic force microscopy (AFM).

Experimental Section

Samples. Undopped, semi-insulating, single-crystal GaAs wafers with orientation (100) were acquired from different sources. Acetone and ethanol (anhydric and analytical grade) used for degreasing were purchased from SDS and used without further purification. Hydrofluoric acid (40% puriss. pro-analysis grade) was purchased from Sigma-Aldrich and diluted to 1% (vol) with deionized water with 18.2 MΩ/cm furnished by a Millipore system. Acetonitrile (99.9%) was obtained from Fluka HPLC grade (less than 0.02% H_2O), and PPA ($C_6H_5PO_3H_2$) (98%) was obtained from Sigma-Aldrich and used as received. The PPA free molecule infrared spectrum was recorded in transmission using a KBr pellet.

After being degreased, the substrates were etched with a 1% solution of hydrofluoric acid, following a procedure described in ref 10. The GaAs substrates, which still contained a very thin layer of oxide,[10] were then immersed for 18 h in a 2×10^{-3} M PPA solution prepared in $(100 - X)$% volume acetonitrile and X% water (with X ranging from 0 to 10). Each sample is designated below by the X% H_2O used for the adsorption. After interaction, all samples were rinsed in acetonitrile, and the excess solvent was evaporated by a nitrogen flow. ATR/MIR samples were all gently sonicated. Only the 10% H_2O samples that were analyzed by XPS and HREELS were compared before and after sonication. The sonicated samples are designated as 10% H_2O sonic.

ATR/MIR. ATR/MIR elements of semi-insulating GaAs (100), which are highly transparent to the infrared radiation in the spectral range of 650−4000 cm^{-1}, were used. Major faces of the ATR/MIR elements, which were 800 μm thick, were cut into 40 × 15 mm rectangles and optically polished in 45° bevelled edges in an isosceles trapezoidal configuration. Spectra were recorded using an FTIRS Magna-IR Nicolet 860 equipped with an MCT detector with a resolution of 4 cm^{-1}. In situ experiments were performed using a homemade Teflon liquid cell with a hole for the introduction and extraction of the solution. Spectra were recorded automatically at predetermined intervals that referred to the moment of the solution introduction. Background was collected for each etched substrate before the PPA interaction. In our experimental conditions, analysis depth was ∼1000 nm,[11] which is much larger than the thickness of the molecular monolayer. All spectra were recorded at room temperature.

XPS. An XSAM800 (KRATOS) XPS spectrometer was used and was operated in fixed analyzer transmission (FAT) mode, with a pass energy of 10 eV and with non-monochromatized Mg Kα and Al Kα X-radiation ($h\upsilon$ = 1253.7 and 1486.7 eV, respectively). The power was set to 130 W. Samples were analyzed in an ultrahigh-vacuum (UHV) chamber (∼10^{-7} Pa) at room temperature, using 0° and 60° analysis angles relative to the normal of the surface. Samples were transferred from the last rinsing solution into the fast introduction chamber under argon atmosphere and were introduced under a pure nitrogen flux. Spectra were recorded by a Sun SPARC Station 4 with Vision software (KRATOS) using increments of 0.1 eV. A Shirley background was used for the baseline subtraction, and the curve fitting for the component peaks was carried out with Voigt profiles (Gaussian/Lorentzian products). No flood gun was used for charge compensation. Binding energies were corrected relative to the GaAs Ga $3d_{5/2}$ equal to 19.1 eV.[10,12] In addition, the modified Auger parameter was used for gallium oxidation state assignment. X-ray source satellites were subtracted. For quantification purposes, sensitivity factors were 0.66 for O 1s, 0.25 for C 1s, 6.3 for As $2p_{3/2}$, 4.74 for Ga $2p_{3/2}$, 0.53 for As 3d, 0.31 for Ga 3d, and 0.39 for P 2p.

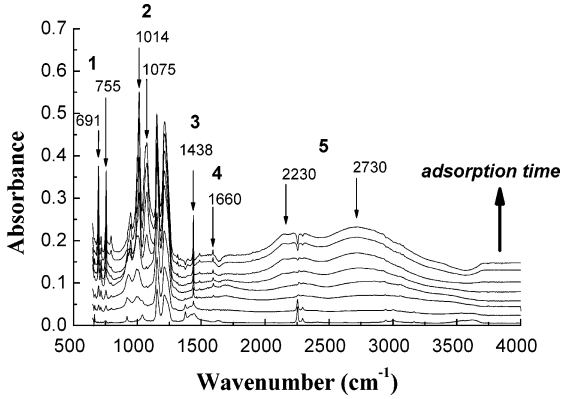

Figure 1. ATR/MIR spectra, recorded in situ, that follow the kinetics of the interaction of PPA with a GaAs (100) surface at different times after the start of the adsorption process. From the bottom to the top: 1 min, 45 min, 1 h and 15 min, 3 h, 3 h and 15 min, 3 h and 30 min, 9 h and 45 min, and 14 h (spectra were arranged to provide a better visual representation). The different wavenumber regions are numbered in accordance with Table 1.

HREELS. Experiments were performed with two different spectrometers: a Leybold-Heraeus ELS-22 and an LK Technologies 2000R, which is described elsewhere.[13,14] Spectra were recorded under ∼10^{-8} Pa using incident electrons of 5 eV. Incidence and analysis angles were in off-specular geometry, which allowed for the analysis of impact interactions and consequently revealed the composition of the layer surface region at a depth of ∼1 nm. Samples were prepared using a fixed protocol and were carried to the UHV chamber under argon and introduced under a pure nitrogen flux.

AFM. AFM images were recorded using a Dimension 3100 SPM with a Nanoscope IIIa controller from Digital Instruments (DI) under ambient conditions. Scanning was performed in tapping mode. A commercial etched silicon probe from DI and a 90 × 90 μm^2 scanner were used.

Results and Discussion

Adsorption Kinetics. The formation of an adsorbed layer during the interaction of the PPA in the solution containing 10% H_2O with the GaAs surface was followed by ATR/MIR in situ using the Teflon cell. Figure 1 shows the spectra recorded at different times after the beginning of the adsorption process: at 1 min, 45 min, 1 h and 15 min, 3 h, 3 h and 15 min, 3 h and 30 min, 9 h and 45 min, and 14 h. The background was recorded relative to the solvent. The spectra indicate not only the accumulation of free molecules but also their chemical transformation due to the interaction with the substrate.

Figure 1 displays the whole spectral range detected from 650 to 4000 cm^{-1}. The assignments of the most important features as well as their relative intensities are given in

(9) Artzi, R.; Daube, S.; Cohen H.; Naaman, R. *Langmuir* **2003**, *19*, 7392.

(10) Rei Vilar, M.; El Beghdadi, J.; Debontridder, F.; Naaman, R.; Ferraria, A. M.; Botelho do Rego, A. M. *Surf. Interface Anal.* **2005**, *37*, 673.

(11) Harrick, N. J. *Internal Reflection Spectroscopy*; Interscience Publishers: New York, 1967.

(12) Wagner C. D.; Naumkin, A. V.; Kraut-Vass, A.; Allison, J. W.; Powell, C. J.; Rumble, J. R., Jr. *NIST X-ray Photoelectron Spectroscopy Database*; NIST Standard Reference Database 20, Version 3.4 (web version); http://srdata.nist.gov/xps/ (accessed 2003).

(13) Dannetun, P.; Schott M.; Rei Vilar M. *Thin Solid Films* **1996**, *286*, 321.

(14) Rei Vilar, M.; Botelho do Rego, A. M.; Lopes da Silva, J.; Abel, F.; Schott, M.; Quillet, V.; Petitjean, S.; Jérôme, R. *Macromolecules* **1994**, *27*, 5900.

Table 1. Major Assignments of Peaks Found in the ATR/MIR Spectra of Adsorbed PPA[a]

regions	wavenumber (cm^{-1})	intensity	assignment[15−17]
1	691 and 720	s	oop deformation of aromatic CH.
	755	m−s	P−C stretching
2	910−1040	w	P−OH in H_2PO_3
	1030−1075*	vs	asym stretching P−O in PO_3H^-
	960−1000*	m	sym stretching P−O in PO_3^{2-}
	970−1125*	s	asym stretching P−O in PO_3^{2-}
	1140−1200	w	associated P═O stretching
	1200−1250	w	free P═O stretching
3	1438	s	aromatic ring in-plane stretching
	1440−1465	m	aliphatic CH sym deformation
4	1660	broad band	associated OH deformation
5	2100−2300	m	OH stretching in P−OH
	2560−2700	m	groups bound by H-bonding.
6	2880−2920	w	aliphatic CH stretching
	3015−3080	w	aromatic CH stretching
7	2600−3700	broad band	OH stretching in H_2O bound by H-bonding
8	3739	w	free hydroxyls

[a] Asterisks indicate the vibrations of the ionic species found in the literature.

Table 1 for the different spectral regions. Peaks in region 2 arise from the first minutes of the interaction. Because of the strong absorbance of the phosphonic and phosphonate species, this region is quite insensitive to variations in the arsenic oxide located around 1060 cm^{-1}.[10,18] A significant contribution of the PPA adsorption also appears in region 3, where one can observe the continuous increase of a narrow peak at 1438 cm^{-1} that is related to the aromatic ring in plane stretching. The broad bands in regions 4 and 5 are characteristic of PPA molecules that are agglomerated by hydrogen bonding, mostly through water molecules.[15] All spectral features indicate the accumulation of PPA molecules near the substrate with time.

After 3−4 h from the beginning of the adsorption, there was an important change in the spectra: new peaks suddenly appeared. Figure 2 shows region 2 of Figure 1 in more detail, comparing it with the corresponding features of the molecules in a KBr pellet. One can note that the peaks between 920 and 950 cm^{-1} and the peak at 1014 cm^{-1}, which are all assigned to P−OH, evolve differently: the bands between 920 and 950 cm^{-1} become much weaker than that at 1014 cm^{-1}. On the other hand, the intensity of the P═O bands at 1151 and 1212 cm^{-1} increases with the time of the interaction. However, the most astonishing event in the kinetics comes from the sudden appearance of the peak at 1075 cm^{-1}. On the basis of other studies, one can assign the peaks at 1014 and 1075 cm^{-1} to P−O stretching modes in the hydrogenophosphonate or phosphonate ions.[17] Their presence can be explained as the deprotonation of PPA in the presence of the water accumulated near the GaAs substrate. Actually, it is well-known that the increase in water concentration in the acetonitrile solution causes a decrease in the pK_a of the acid, which dissociates.[19,20]

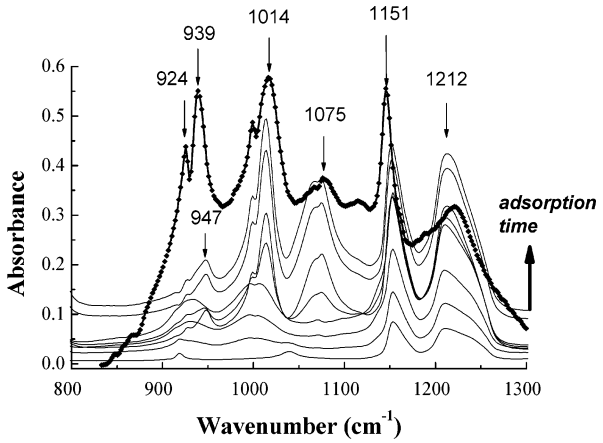

Figure 2. Detail of the in situ ATR/MIR spectra (shown in Figure 1) in the phosphorus−oxygen region between 850 and 1300 cm^{-1}. The transmission spectrum of the free molecule in a KBr pellet is displayed as a dark line with diamond symbols.

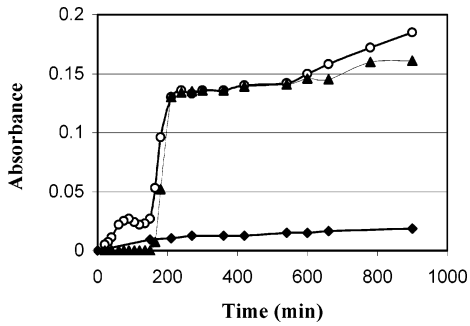

Figure 3. Absorbance intensity of the peaks at 691 cm^{-1} (○) and 1075 cm^{-1} (▲) in 10% water solutions and of the peak at 691 cm^{-1} in an anhydric solution (◆) versus time.

These observations are correlated with a rapid, continuous intensity increase of the narrow peaks associated with the phenyl groups of the acid, which are related to aromatic C−H out-of-plane (oop) deformations at 691 cm^{-1} and related to ring in-plane stretching modes at 1438 cm^{-1}.

The kinetics associated with this adsorption process are presented in Figure 3, in which the absorbance of the peaks at 691 and 1075 cm^{-1} in 10% water solutions as well as that of the peak at 691 cm^{-1} in an anhydric solution are displayed versus the time. Here, one can clearly see the important role played by water in the adsorption process. In the case of the anhydric solution, a plateau of absorbance (Langmuir-type adsorption) on the order of 10^{-3} is attained after ~3 h of interaction, whereas, for the 10% H_2O solution, the plateau is on the order of 10^{-1} after the same time. Furthermore, one can note that, in the plateau, there is a superposed linear increase of PPA molecules. This tendency, still stronger after 10 h from the start of the interaction, is associated with the accumulation of PPA molecules in the liquid solution near the GaAs surface (the length of the evanescent wave is on the order of 1000 nm). Between 0 and 200 min after the start of the adsorption, the absorbance of the peak at 691 cm^{-1} in the solution with water is always higher than that of the same peak in the anhydric solution. In contrast, during the same period, the intensity of the peak at 1075 cm^{-1} is zero; after 150 min from the start of the interaction, its absorbance abruptly increases attaining a value higher than 10^{-1}. This confirms that the feature at 1075 cm^{-1} must correspond to a new chemical entity. The most probable candidates are, as mentioned above, the hydrogenophosphonate ion PO_3H^- and the phosphonate PO_3^{2-} ions, a prediction that is supported by the decrease in the

(15) Socrates, G. *Infrared Characteristic Group Frequencies*, 2nd ed.; John Wiley & Sons: New York, 1994.
(16) Thomas, C.; Chittenden, R. A. *Spectrochim. Acta* **1964**, *20*, 467.
(17) Ohno, K.; Mandai, Y.; Matsuura, H. *J. Mol. Struct.* **1993**, *298*, 1.
(18) Lenczycki, C. T.; Burrows, A. *Thin Solid Films* **1990**, *193−194*, 610.
(19) Espinosa, S.; Bosch. E.; Rosés M. *Anal. Chem.* **2002**, *74* (15), 3809.
(20) Buckenmaier, S. M. C.; McCalley, D. V.; Euerby, M. R. *J. Chromatogr., A* **2003**, *1004*, 71.

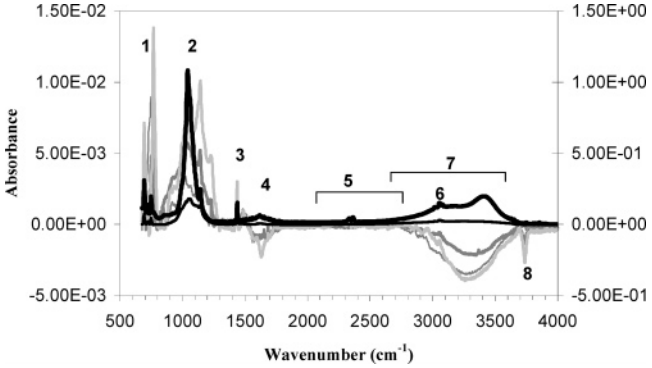

Figure 4. ATR/MIR spectra of PPA adsorbed on GaAs (100) surfaces from acetonitrile solutions containing different water contents: 0 (bold light gray), 1 (gray), 3 (bold gray), 5 (black), and 10% (bold black). The spectra of 5 and 10% H_2O samples are reported in the secondary axis on the right. The different wavenumber regions are numbered in accordance with Table 1.

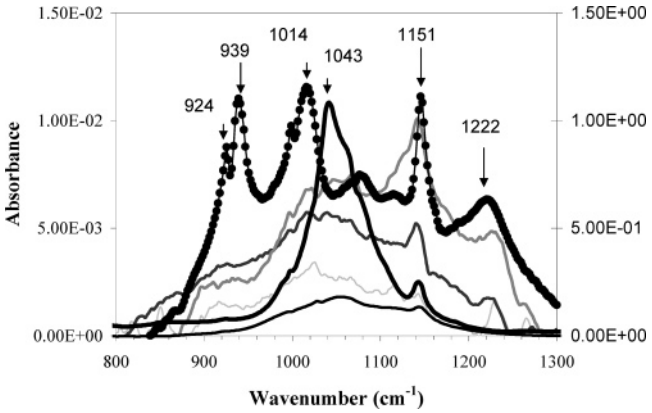

Figure 5. ATR/MIR spectra recorded in the region of the phosphorus−oxygen bonds, magnified from region 2 of Figure 4; 0 (bold light gray), 1 (gray), 3 (bold gray), 5 (black), and 10% (bold black) H_2O contents are shown. The spectra of 5 and 10% H_2O samples are reported in the secondary axis on the right. The transmission spectrum of the free molecule in a KBr pellet is displayed as a line with solid circles.

peak absorbance related to P−OH. However, the P−O vibrations of PO_3^{2-} and PO_3H^- are assigned to the same spectral region between 950 and 1100 cm^{-1}, and it is therefore difficult to elect one of them.[21]

Layer Characterization. ATR/MIR spectra were also recorded with dried GaAs surfaces that were examined after interaction with PPA in acetonitrile solutions containing variable amounts of water. Adsorption times were longer than the kinetics plateau threshold estimated above. Figure 4 presents spectra corresponding to 0, 1, 3, 5, and 10% H_2O samples. The spectral regions are also numbered according Table 1.

One can easily observe a remarkable difference in the region assigned to P−O bonds. This region, detailed in Figure 5, involves a strong overlapping of the different P−O contributions. The broadening is related to intermolecular interactions that are mainly due to hydrogen bonding. As observed in the in situ kinetics, these bands markedly change in intensity and shape with the percentage of H_2O, revealing the presence of phosphonic ionic species.

Changes in region 2, in correlation with the water content in the solution, indicate the mechanism of the formation of the PPA layer. In fact, in the case of the samples prepared with an H_2O content lower than 5%, region 2 has clear contributions of P−OH (at 920 and 1020 cm^{-1}) and P═O (at 1145 cm^{-1}), which are assigned to molecules that are mostly associated through hydrogen bonding. In contrast, at approximately 1230 cm^{-1}, a weak peak is present for low percentages of H_2O and completely absent for the 5 and 10% H_2O samples. This feature is assigned to P═O stretching in the free molecules. For the 5% H_2O sample, a strong increase in the absorption band contribution is located at 1040 cm^{-1}. This is reinforced in the sample with 10% H_2O. As mentioned above, this band exists in spectra of organophosphonic acid containing PO_3^{2-} and PO_3H^- in which the contributions are hardly distinguishable.[17] However, the observation of a band located at 1145 cm^{-1}, which is typical of P═O bonds, should be related to the hydrogenophosphonate. On the other hand, the relative contribution of the modes related to P−OH and P═O located around 920 and 1145 cm^{-1} are very weak in the spectra of the 5 and 10% H_2O samples, confirming the dissociation of the molecule for solutions with high percentages of H_2O. This leads to the conclusion that phosphonate ions (PO_3^{2-} and/or PO_3H^-) are constituents of the layer and evoke polyionic layer formation for 5 and 10% H_2O solutions.

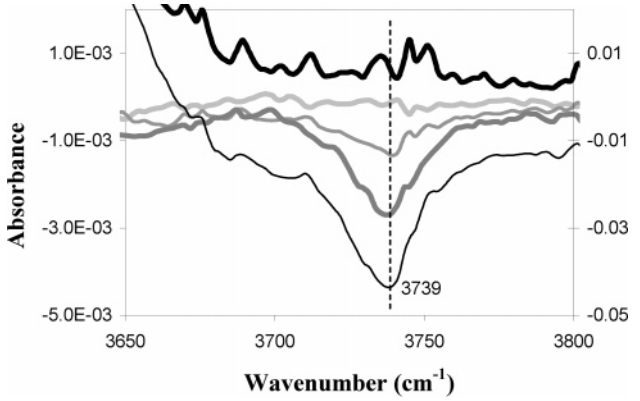

Figure 6. ATR/MIR spectra in the region of the hydroxyl groups; 0 (bold light gray), 1 (gray), 3 (bold gray), 5 (black), and 10% (bold black) H_2O contents are shown. The spectra of 5 and 10% H_2O samples are reported in the secondary axis on the right.

The major difference between these spectra and those obtained in the liquid phase presented in Figure 2 is the low contribution of the peaks corresponding to the P−OH and P═O features in the free molecules relative to the band appearing around 1045 cm^{-1}. This result confirms that the water bound to the surface reduces the pK_a of the PPA, which was already concluded from the kinetics studies (see above). These peaks almost disappear when the samples are sonicated and liberated from physisorbed molecules.

The broad bands in regions 4 and 7, shown in Figure 4, correspond to molecules associated through hydrogen bonds. Water attaches (positive intensity) or leaves the surface (negative intensity) of the GaAs ATR element during the different adsorption experiments. In the case of solutions containing 0, 1, and 3% H_2O, the "bound water" present on the substrate disappears following the adsorption. This is correlated with the disappearance of surface hydroxyls from the substrate.

The evolution of region 8 in Figure 4 suggests different mechanisms, depending on the water concentration. Figure 6 shows this region of the spectrum in detail. For the 0% H_2O solution, no modification could be observed

(21) Barja, B. C.; Tejedor-Tejedor, M. I.; Anderson, M. A. *Langmuir* **1999**, *15*, 2316.

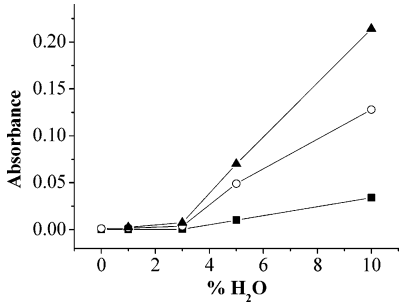

Figure 7. Absorbance of the most pronounced bands of PPA recorded in ATR/MIR versus the water content in the solution: CH oop at 691 cm^{-1} (▲), CH bending at 1438 cm^{-1} (○), and CH stretching at 3056 cm^{-1} (■). The lines serve as visual guides.

in the hydroxyl region. In contrast, for the 1, 3, and 5% H_2O samples, there are negative bands of increasing intensity with minima located at 3739 cm^{-1}, showing that free or geminated hydroxyl groups are consumed during the interaction. In the particular case of the 10% H_2O sample, the absence of a peak in this region shows the low involvement of hydroxyl groups on the layer formation. In contrast, one can observe the appearance of "bound water" on the surface after the adsorption from solutions containing 5 and 10% H_2O. This is also accompanied by an enormous increase in the absorbance corresponding to the PPA ionic species (region 2).

The adsorption of PPA could also be followed through the evolution of the phenyl vibrations modes. In Figure 7, the absorbance of the three most typical peaks at 691, 1438, and 3056 cm^{-1} (see Table 1) versus the percentage of H_2O is shown. For 1438 cm^{-1}, for instance, the absorbance increases ~100 times between 3 and 10% water but is almost independent of the water concentration for samples prepared with water contents lower than 3% H_2O.

Here, XPS spectroscopy plays an important role for a more thorough analysis of the adsorbed PPA layers. Actually, the ATR/MIR observations are consistent with the XPS results, which also reveal a dramatic increase in PPA adsorption for the 5 and 10% H_2O solutions. Figure 8 shows the carbon (C 1s) and phosphorus (P 2p) regions, after satellite subtraction, for five of the studied samples: 0, 3, 5, and 10% H_2O and 10% H_2O sonic. The P 2p peak, at 133.2 ± 0.3 eV, which is a doublet with a separation of 0.87 eV, is practically absent in 0 and 3% H_2O samples but is very intense in 5 and 10% H_2O samples. This peak is on the tail of the As 3p region (As $3p_{3/2} \approx 140$ eV). The C 1s peak, which appears superposed on an Auger structure (As LMM for the Al anode and as Ga LMM for the Mg anode), has the same behavior. For samples in which the amount of C 1s contribution is very small (0−4%), the peaks are very weak, with areas difficult to compute, and are therefore calculated with relatively large errors. In contrast, for the 5 and 10% H_2O samples, the C 1s peaks are strong. For the 10% H_2O sonic sample, the intensities of the C 1s and P 2p peaks decrease, showing that molecules are removed through sonication. In contrast, the As 3p peaks are much less intense in the 5 and 10% H_2O samples, confirming a higher thickness for samples prepared with higher percentages of H_2O, but they become stronger after sonication, which indicates that a part of the layer is eliminated.

Figure 9 presents quantitative results expressed in the atomic percentages of the different elements versus the percentage of H_2O. One can note that both Ga 2p and As 2p signals, which are fairly constant for H_2O contents below 5%, substantially decrease for 5% H_2O and maintain approximately the same level for 10% H_2O. This results from the global increase in the coverage of the substrate by the acid molecules. However, the much greater decrease of the signal As 2p compared to that of Ga 2p can only be explained by the selective dissolution of arsenic oxide.[10] Actually, in past studies, water was found to be of major importance in the selective dissolution of arsenic oxides, creating gallium-enriched GaAs surfaces even in the absence of light.[10,22,23] The As 3d signal does not decrease as much as that of As 2p because the As 3d signal results from electrons originated deep underneath the substrate and is therefore less sensitive to the extreme surface region. It is worth emphasizing here that, in these samples, in which the XPS Ga 3d and Auger $L_3M_{45}M_{45}$ regions present two components each, the modified Auger parameters are 1085.0 ± 0.3 and 1082.0 ± 0.3 eV, which are very close to the values found for the gallium in GaAs and for the gallium in powdered Ga_2O_3,[24] respectively. Returning to Figure 9, the P 2p and C 1s XPS atomic percentages are represented in scales differing by a factor 6, which is the stoichiometric ratio C/P in PPA. The curves basically overlap following the stoichiometric normalization, indicating that the contribution of the aliphatic contaminants to the carbon signal is practically negligible.

The quantitative results for the most important atomic ratios are displayed in the appendix.

Atomic ratios C 1s/Ga 3d and P 2p/Ga 3d were used to estimate the layer thickness. Values for the electron escape depth λ were computed from an expression proposed by Tanuma et al. for the inelastic mean free path: the modified predictive formula TPP-2M (from the modified Bethe equation).[25]

$$\lambda = E/\{E_p^2[\beta_M \ln(\gamma E) - (C/E) + (D/E^2)]\} \qquad (1)$$

in which E is the photoelectron kinetic energy, E_p is the free electron plasmon energy, and β_M, γ, C, and D are parameters related to material properties.

When flat substrates and homogeneous gallium and acid density in depth are assumed, the only parameters to be fitted are the organophosphorus layer thickness and the ratio c_X/c_{Ga} between the atomic density of X in the layer, X being carbon or phosphorus, and the atomic density of Ga in the substrate. The following expression for the XPS atomic ratio, X/Ga, is obtained as

$$\frac{X}{Ga}(Y, \theta) = \frac{c_X}{c_{Ga}} \frac{1 - \exp\left(-\frac{\ell_{acid}}{\lambda_X(Y)\cos(\theta)}\right)}{\exp\left(-\frac{\ell_{acid}}{\lambda_{Ga\ 3d}(Y)\cos(\theta)}\right)} \qquad (2)$$

in which X is P or C, c_X is the density of X in the acid film, c_{Ga} is the density of gallium in the substrate, θ is the analysis angle with the surface normal, and $\lambda_X(Y)$ is the inelastic mean free path of the photoelectrons of P 2p and C 1s in the PPA film for both anodes Y (Mg and Al). The fitting of eq 2 to the experimental results for the C/Ga and P/Ga atomic ratios was done using the least-squares method.

(22) Massies, J.; Contour, J. P. *Appl. Phys. Lett.* **1985**, *46*, 1150.
(23) Kirchner, C.; George, M.; Stein, B.; Parak, W. J.; Gaub, H. E.; Seitz, M. *Adv. Funct. Mater.* **2002**, *12* (4), 266.
(24) Mizokawa, Y.; Iwasaki, H.; Nishitani, R.; Nakamura, S. *J. Electron Spectrosc. Relat. Phenom.* **1978**, *14*, 129.
(25) Tanuma, S.; Powell, C. J.; Penn, D. R. *Surf. Interface Anal.* **1994**, *21*, 165−176.

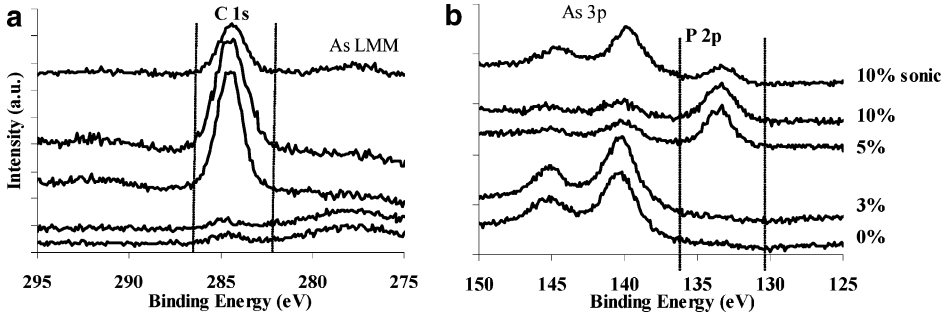

Figure 8. XPS C 1s (a) and P 2p (b) spectral regions. From bottom to top, data correspond to 0, 3, 5, and 10% H_2O and 10% H_2O sonicated samples after adsorption. The spectra were normalized and separated for the sake of clarity. The spectra were recorded, using Al Kα radiation in a direction that was normal to the surface. The source satellites were subtracted, and the charge shift was corrected.

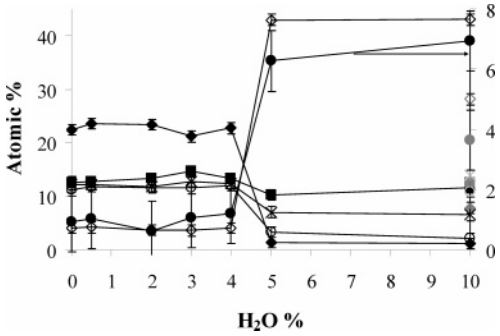

Figure 9. XPS Atomic percentages for the main elements of X% H_2O samples versus X: As 2p (◆), As 3d (○), Ga 2p (■), Ga 3d (×), C 1s (◇) and P 2p (●). The light gray symbols correspond to 10% H_2O sonic samples. A secondary y-axis is used for the P 2p atomic concentration. The lines serve as visual guides. The results were obtained with an Al Kα X-ray source at an 0° analysis angle.

The following conditions were used as constraints to the fitting:

$$0.1 \leq \frac{c_P}{c_{Ga}} \leq 0.3 \text{ and } c_C = 6c_P \qquad (3)$$

The first condition comes from the assumption that the atomic density of both phosphorus and gallium in the PPA film and in the substrate should have the same order of magnitude of the bulk densities. Actually, taking into account the bulk properties, the gallium density in GaAs is 0.03677 mol cm^{-3},[26] and, in pure Ga_2O_3, the density is 0.064 mol cm^{-3}.[27] For PPA, the phosphorus bulk density equals 0.0093 mol cm^{-3};[28] hence, the expected value for c_P/c_{Ga} ranges from 0.15 to 0.26. Because of porous substrate, for instance, or especially strong or weak interactions between molecules in the film, a wider range from 0.1 to 0.3 was allowed for c_P/c_{Ga} to ensure that different ratios could be found. However, using these values, no fitting of the experimental values for 5 and 10% H_2O samples was achieved. One must conclude then that the assumptions made concerning the flatness of both the substrate and the organic layer are not realistic. This also corroborates the fact that the selective disappearance of arsenic oxide must introduce a degree of roughness on the surface, which can be confirmed by AFM.

The AFM images shown in Figure 10 correspond to 0, 3, 5, and 10% H_2O samples. Two different height/color scales were used for the images: 5 nm (0 and 3%) and 100 nm (5 and 10%). The topography of the 0% sample reveals the presence of features, having heights in the range of 8−13 nm, on top of a clean substrate that is characterized by a local mean roughness value (measured between the aggregates), $R_q \approx 0.25 \pm 0.03$ nm, which is typical of the reference substrate ($R_q \approx 0.26 \pm 0.03$ nm). The topography of the 3% H_2O sample shows a uniform coverage of the substrate and grain formation with typical diameters of 40−70 nm. The overall mean roughness of the sample is 0.50 ± 0.05 nm. As the water content increases to 5%, aggregates are observed, and a granular structure, as in the 3% H_2O sample, remains in both the aggregates and the underlying film. This granular texture is clearly displayed in the inset, which corresponds to the rectangular regions illuminated in the image for which the color/height scale was set to 20 nm (×5). This sample is characterized by an overall mean roughness value, $R_q \approx 13 \pm 2$ nm, and a local mean roughness value, $R_q \approx 7 \pm 1$ nm. The topography of the 10% H_2O sample reveals a coalescence of the individual aggregates that were observed in the 5% H_2O sample. This leads to a decrease in

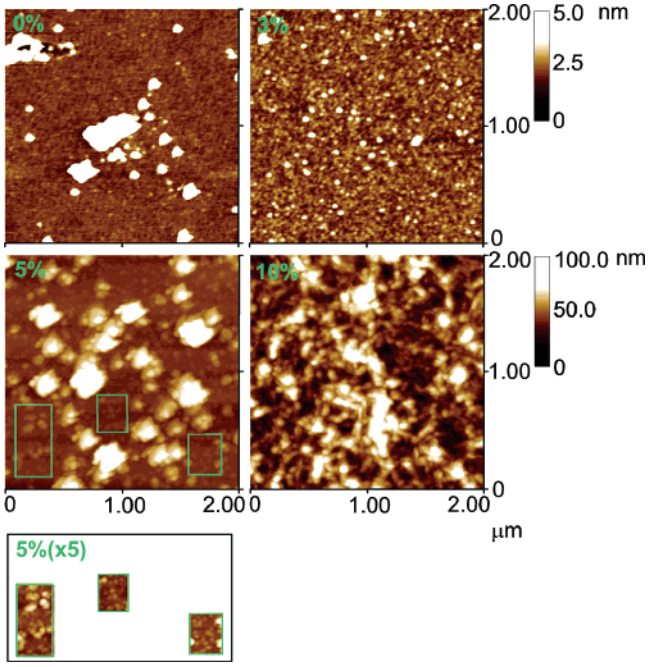

Figure 10. AFM topographic images for 0, 3, 5, and 10% H_2O samples. Two height/color scales were used for the images: 5 nm for the 0 and 3% H_2O samples and 100 nm for the 5 and 10% H_2O samples. The inset corresponds to the rectangular regions enlightened in the 5% H_2O image, for which the color/height scale is set to 20 nm.

(26) GaAs MMIC Reliability Assurance Guideline for Space Applications. http://parts.jpl.nasa.gov/mmic/3-I.PDF.
(27) *Handbook of Chemistry and Physics*, 58th ed.; Weast, R. C., Ed.; CRC Press: Boca Raton, FL, 1977.
(28) Alfa Aesar Home Page. http://www.alfa-chemcat.com

Scheme 1. Model Used for Fitting P/Ga and C/Ga Atomic Ratios

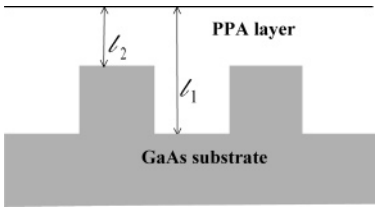

Table 2. Density Ratios (c_P/c_{Ga}), Coverage Fraction (f), and Layer Thickness of PPA Layers Computed from Equation 4 for Samples Prepared from Solutions Containing Several Water Percentages[a]

H_2O %	c_P/c_{Ga}	f	l_1 (nm)	l_2 (nm)	R_q (nm)
0	0.15	0	0	0.8	0.25 ± 0.03
0.5	0.15	0	0	0.8	
2	0.15	0	0	0.8	
3	0.15	0	0	0.8	0.50 ± 0.03
4	0.15	0	0	0.8	
5	0.30	0.71	15	0.8	7 ± 1
10	0.30	0.70	20[b]	0.8	8 ± 1
10 (sonic)	0.30	0.47	5.1	0.8	

[a] Roughness values are indicated. [b] This value means that the thickness is larger than 15 nm. A precise value cannot be given.

the overall R_q to 8 ± 1 nm. The granular structure is still observed throughout the sample.

These results lead to another model displayed in Scheme 1 to fit the XPS results: This second model introduces a regular roughness in the gallium substrate (either gallium arsenide or gallium oxide, which are assumed to have the same gallium atomic density). The PPA layer is not flat and is constituted by two layers of two different thickness, ℓ_1 and ℓ_2. With this model, neglecting shadow effects and introducing the fraction of the surface covered by the thicker layer (f), we obtain:

$$\frac{X}{Ga}(Y,\theta) = \frac{c_X}{c_{Ga}}\left[f\left[1-\exp\left(-\frac{\ell_1}{\lambda_X(Y)\cos(\theta)}\right)\right]+(1-f)\left[1-\exp\left(-\frac{\ell_2}{\lambda_X(Y)\cos(\theta)}\right)\right]\right]\Bigg/\left[f\exp\left(-\frac{\ell_1}{\lambda_{Ga}(Y)\cos(\theta)}\right)+(1-f)\exp\left(-\frac{\ell_2}{\lambda_{Ga}(Y)\cos(\theta)}\right)\right] \quad (4)$$

Eight different experimental results are available, on the basis of Ga 3d, for each sample (P/Ga and C/Ga) with two different anodes (Al and Mg) and two different analysis angles (0 and 60°). Four different parameters (c_P/c_{Ga}, f, ℓ_1, and ℓ_2) can be found by fitting eq 4 to them. Best fitting parameter values are shown in Table 2, which also displays the local mean roughness value, R_q.

After fitting, it is interesting to note that the density ratios c_P/c_{Ga} for samples prepared with H_2O contents of less than 5% are lower (0.15) than those obtained for the 5 and 10% H_2O samples (0.30). In the samples prepared with water concentrations of 0−4%, only the thin layer exists with a thickness (ℓ_2) of 0.8 nm on the order of a monolayer. For the 5 and 10% H_2O samples, a second thick layer of 15 and 20 nm, respectively, is formed on the monolayer. However, the density of this layer is approximately two times higher than that of the monolayer. This fact suggests a more compact system with stronger cohesive interactions existing between the components.

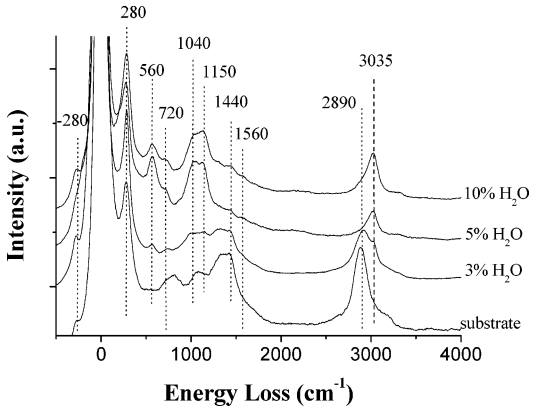

Figure 11. HREELS vibrational spectra of the raw substrate and of the 3, 5, and 10% H_2O sonic samples. The spectra were recorded in off-specular geometry with an incident electron energy of 5 eV.

In contrast, for the sonicated sample, both ℓ_1 and the corresponding surface fraction are lower.

Nevertheless, the parameters in Table 2 do not reproduce experimental values for the ratios of C/Ga 2p (or P/Ga 2p) in the 5 and 10% samples. In fact, with the model in Scheme 1, values for those XPS atomic ratios should increase. Instead, however, they decrease. This result is consistent with the presence of Ga mixed in the organic layer. However, the number of parameters to fit a model containing oxidized gallium, both in the layer and in the substrate, with different atomic densities becomes so large that physically meaningful values cannot be obtained. The model in Scheme 1 is at least compatible with the quantitative results if some oxidized gallium is added to the layer.

In addition to ℓ_1, ℓ_2, f, and the phosphorus atomic density in the layer, fitting the model in Scheme 1 to the XPS ratio O/P demands extra parameters: oxygen atomic densities in both the oxide and the layer and oxide layer thickness. Therefore, it is not possible to find all the parameters by a fitting procedure. Furthermore, no parameter combination with $c_O/c_P = 3$ (the stoichiometric ratio in PPA) in the layer yields computed values similar to the experimental ones. However, with $c_O/c_P = 3.3-3.5$, good agreement is obtained when one assumes that $c_{O(\text{in the oxide layer})}/c_{P(\text{in the organic layer})} = 10$ and that the oxide layer is ~2 nm thick. In the sonicated sample, because the fraction of the substrate covered by a thin layer increases and the thickness ℓ_1 of the thicker layer decreases relative to the nonsonicated one, the relative importance of gallium oxide in the substrate should increase. In fact, the O/P ratio increases to ~6 for an analysis angle that is 0° relative to normal and ~5 for a 60° analysis angle. At the same time, one can observe an important decrease in the relative amount of oxidized gallium to less than 20% of the amount existing in the nonsonicated sample. In addition, the As/Ga ratio increases. Simultaneously, the ratios of C/Ga and P/Ga decrease. These observations show that, as a result of the sonication, oxidized gallium decreases together with the organic material. This strongly suggests that Ga^{3+} ions, together with H_3O^+ ions, are present in the organic layer, acting as counterions of the PPA ionic species (hydrogenophosphonate and phosphonate). The presence of these electrostatic forces of cohesion agrees with the higher density of layers that are produced when the 5 and 10% H_2O samples are used.

HREELS spectroscopy was used to characterize the extension of the PPA coverage regions on the GaAs surface and those of contamination. Figure 11 shows HREELS

vibrational spectra for three samples and for the substrate that was obtained for an incident energy of 5 eV in off-specular geometry.

Different features can be identified and assigned in all spectra displayed in Figure 11. In the very low energy loss domain, one can find peaks resulting from the excitation of the well-known, characteristic surface phonon of GaAs (100) around 280 cm^{-1} along with its symmetric energy gain relative to the elastic peak.[29] The next feature at 560 cm^{-1}, present in all of the samples except that of the bare substrate, is assigned to the benzene ring deformation modes but should also include some contribution from the double scattering of the GaAs (100) surface phonon. The weak feature around 720 cm^{-1}, which is also observed in ATR/MIR spectra, is assigned to the oop deformations of the aromatic C−H bonds. This oop vibration, with a transition moment perpendicular to the plane of the phenyl ring, has often been used to infer the orientation of the phenyl functions relative to the substrate.[30] Using the selection rules for the dipole−electron mechanism, one can observe that this mode is not increased in specular geometry. However, its differential cross-section decreases with the incident electron energy, which shows the dipolar character of the interaction. This is consistent with the phenyl groups being mainly oriented perpendicular to the surface. Around 1100 cm^{-1}, an intense and broad peak appears, as was described above in ATR/MIR, corresponding to several vibration modes of the phosphorus−oxygen bond in the PPA and its ionic forms. For water contents of less than 4%, the features are comparable to the bands in ATR/MIR. For higher water contents (5 and 10%), the sonic spectra exhibit two strong contributions centered at 1040 and 1150 cm^{-1}, as seen in the infrared spectra, which are assigned, in the literature,[15] to the phosphorus−oxygen vibrations in the hydrogenophosphonate. A low contribution that is also observed in this same region of the bare substrate spectrum is assigned to the As−O stretching modes.[10]

The band centered at 1440 cm^{-1} in all of the samples, includes contributions from two sources: (1) a narrow contribution corresponding to the characteristic aromatic ring in-plane stretching of the P−ϕ bond (ϕ being the phenyl group), already found in the ATR/MIR spectra at 1438 cm^{-1}; and (2) a broad contribution corresponding to the asymmetric deformation mode of the CH aliphatic bonds from eventual contaminations.

However, the broad contribution is very low in 5% and 10% H_2O sonic samples but is much higher in the 3% H_2O sample, which attests to the presence of surface contamination. The same conclusion can be drawn from the higher loss energy domain around 3000 cm^{-1}, corresponding to the C−H stretching modes. Peaks at 2890 cm^{-1} are typical of the C−H bonds of aliphatic hydrocarbons, whereas those around 3035 cm^{-1} correspond to the aromatic C−H bond stretching of the PPA. It is clear that the aliphatic feature appearing in the different spectra only results from contaminants. This is particularly evident in the substrate spectrum. On the other hand, the spectra of the 5 and 10% H_2O sonic samples do not exhibit strong aliphatic contributions, indicating that chemisorption either expels or mostly covers the aliphatic contaminants. Interestingly, in the case of the 3% H_2O sample, aliphatic and aromatic contributions have approximately the same relative weight, which clearly shows that the parts of the substrate uncovered by the acid appear to be contaminated, as is shown in the substrate spectrum. This is likely due to the spontaneous tendency of the substrate to minimize its surface energy by contamination adsorption. In fact, free GaAs (100) and phenyl-covered GaAs (100) surfaces have very different surface energies. For GaAs (100), the surface energy is 2.2 J/m^2.[31] No value of surface energy was found in the literature for GaAs (100) surfaces covered with PPA, but one can assume that it must be of the same order of magnitude as that of polymers that contain phenyl groups, such as polystyrene, for instance, for which the surface energy is ∼0.03−0.05 J/m^2.[32] One should infer from the difference of these values that uncovered surfaces of GaAs (100) are more easily contaminated than covered ones. In brief, one can consider the different surfaces studied here as being patchworks of two types of regions: those covered by PPA and those covered by aliphatic contaminants. This is mainly true for the 0−4% H_2O samples (in Figure 11, only the 3% H_2O sample is displayed for the sake of clarity), in which both contributions are present. In contrast, in the spectra of the 5 and 10% H_2O sonic samples, the main component is clearly the aromatic one.

In the HREELS studies, discrepancies appear in some of the samples between the electron nominal energy, imposed by the voltage difference between the filament central point and the sample surface, and the real incident electron energy, which is measured from the elastic peak until the cutoff of the spectra where the kinetic energy becomes zero. This is an indication of the charging of the surface.[33] The difference in energy is approximately +1.5 eV for the 5% sample, and approximately −0.5 eV for all of the other samples from 0 to 4% H_2O and for the 10% H_2O sonic. The difference of ∼1.5 eV is due to a significant negative charge accumulation, which results from the poor conductivity of the layer that has electron traps. This indicates that the organic layer is thick, much more so than a single monolayer. For the 10% H_2O sample (nonsonicated), the effect was even more dramatic: with a nominal energy of 2 eV, no spectrum could be obtained. This effect implied that this sample was sonicated.

Conclusions

The techniques used in this study have different analysis depths. Whereas ATR/MIR probes depths of up to 1000 nm, XPS probes depths up to only ∼10 nm, HREELS is sensitive to a depth of ∼1 nm, and AFM microscopy only probes the surface morphology. The combination of those methods allowed us to obtain detailed information on the adsortpion of PPA, its kinetics, the nature of its bonding to the surface, and the morphology of the adsorbed layer.

The kinetics of the formation of PPA layers shows considerable differences, depending on the amount of water present in the solution used for adsorbing the organic layer.

In the case of anhydric solutions, the layer thickness is of the same order of magnitude of the monolayer. For water contents less than 5%, the interaction of PPA with the surface consumes surface hydroxyls, forming interfacial covalent bonds. Actually, the adsorption of the molecules is accompanied by the disappearance of the IR band that corresponds to free basic hydroxyl groups at 3739 cm^{-1}. The adsorption is mainly controlled by a mechanism in which PPA molecules interact with the surface hydroxyls (having a basic character) as a first

(29) Dubois, L. H.; Schwartz, G. P. *J. Electron. Spectrosc. Relat. Phenom.* **1983**, *29*, 175.

(30) Rei Vilar, M.; Horowitz, G.; Lang, P.; Pellegrino, O.; Botelho do Rego, A. M. *Adv. Mater. Opt. Electron.* **1999**, *9*, 211.

(31) *Freiberger General Specifications*; Freiberger Compound Materials GmbH: Freiberg, Germany, 2000.

(32) Clancy, T. C.; Jang, J. H.; Dhinojwala, A.; Mattice, W. L. *J. Phys. Chem. B* **2001**, *105* (46), 11493.

(33) Pellegrino, O.; Rei Vilar, M.; Horowitz, G.; Botelho do Rego, A. M. *Mater. Sci. Eng.* **2002**, *C22*, 367.

Scheme 2. Acid−Base Mechanism of the Chemisorption of PPA on GaAs Surfaces

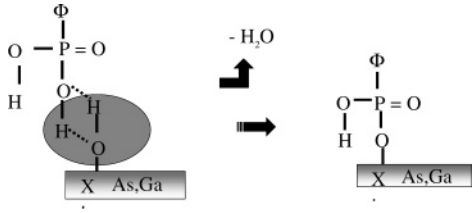

step of the condensation reaction with the formation of a water molecule, which leads to covalent bonding with the substrate.[9] This mechanism is consistent with the formation of a monolayer. This reaction mechanism is shown in Scheme 2. PPA adsorbs mostly on Brønsted basic sites, forming low-density monolayers.

During the adsorption, the GaAs surface becomes richer in Ga because of the dissolution of the arsenic oxide. This suggests that the adsorption of the phosphonic acid is preferentially held on gallium oxide sites, which leads to the formation of P−O−Ga bonds. Clearly, water is required so that adsorption can take place. In reality, for the 0% H_2O sample, only a small amount of molecules is adsorbed, but the rate of adsorption increases with the water concentration. AFM measurements of the roughness for these different samples are consistent with a very schematic model involving a single low-density monolayer covering the substrate.

For water contents of 5% or more, a dramatic increase in the thickness of the layer is observed. The spectral intensity of the peaks corresponding to the phenyl groups is particularly enhanced, which indicates the presence of a thick adsorbed layer. The aggregation of phenylphosphonate ions occurs, and thicker layers are then formed. This reveals, in room conditions, the existence of an aqueous interphase near the GaAs surface where PPA molecules first concentrate and then dissociate, adsorbing to the surface. Here, water plays the role of a driving force in the layer formation. The analysis of the layers after sonication and solvent evaporation indicates the presence of a different state of the protonation of PPA, which is most likely the hydrogenophosphonate ion that concentrates on the surface with H_3O^+ and Ga^{3+} ions. A very schematic model, for 5 and 10% H_2O sonic samples, is fit by two domains: one (approximately one-fourth of the total area) covered by a PPA monolayer and the other one (approximately three-fourths of the total area) covered by a multilayer structure mixed with gallium ions. The XPS O/P ratio is reproduced by the same schematic model if the atomic O/P ratio in the layer is larger than 3, which corresponds to the stoichiometric ratio. This indicates the intercalation in the layer of either the water molecules or, most probably, the H_3O^+ ions acting as counterions of the PPA ionic forms. In fact, the presence of positive charges is needed to associate the anions produced. In addition, the disappearance of arsenic oxide compared to that of gallium oxide suggests that the adsorption of the thick layer is made on the monolayer that is adsorbed on the gallium sites.

The HREELS analysis of the carbon species in the extreme surface shows that, for water contents of less than 4%, the substrate is only partially covered with phenyl groups. In contrast, for water contents greater than 5%, the substrate is totally covered by the phenyl groups. In the HREELS spectra of the samples made from the solution containing 10% water, the charging effect is consistent with very thick organic layers, in which electrons are efficiently trapped. For the 10% H_2O sonicated samples, charge effects are much less important, which indicates a thinner organic layer.

Table 3. XPS Atomic Ratios for the Main Elements Present in the Surface

			H_2O %						
	anode	angle (°)	0	2	3	4	5	10	10 (sonic)
C 1s/Ga 3d	Mg	0	0.30	0.28	0.28	0.24	7.7	7.6	2.3
		60	0.98	0.50	0.78	0.72	9.7	10.5	4.4
	Al	0	0.33	0.31	0.28	0.33	6.1	6.6	2.0
		60	0.68	0.65	0.76	0.85	8.1	7.9	3.8
C 1s/Ga 2p	Mg	0	0.33	0.27	0.28	0.26	4.1	4.0	2.0
		60	1.28	0.57	0.96		5.6	4.9	3.5
	Al	0	0.32	0.28	0.25	0.31	4.2	3.7	2.2
		60	0.83	0.71	0.79	0.91	5.5	4.4	3.5
Ga_{ox} 3d/ Ga_{nox} 3d	Mg	0	0	0	0	0	1.4	1.2	0.16
		60	0	0	0	0	4.2	2.7	0.31
	Al	0	0	0	0	0	0.9	0.66	0.15
		60	0	0	0	0	3.1	1.7	0.34
O 1s/P 2p	Mg	0	4.4	3.7	3.6	1.8	4.3	4.6	6.2
		60	5.9	3.4	3.9	3.4	4.0	3.9	4.6
	Al	0	4.2	6.1	3.6	2.8	4.6	4.2	6.4
		60	7.1	3.9	2.6	3.2	4.2	4.0	5.0
As/Ga (3d)	Mg	0	0.97	1.0	0.91	1.0	0.33	0.30	0.85
		60	1.2	1.1	1.1	1.1	0.14	0.13	0.84
	Al	0	0.91	1.0	0.90	1.0	0.47	0.32	0.78
		60	0.96	1.2	1.00	1.1	0.22	0.18	0.65
As/Ga (2p)	Al	0	1.8	1.8	1.5	1.7	0.13	0.10	0.62
		60	2.1	2.0	1.8	2.1	0.06	0.05	0.51

This study suggests that phosphonic acids are excellent candidates for grafting molecular assemblies onto gallium arsenide surfaces. One must also conclude that the formation of monolayers or of thicker layers containing phosphonate and/or hydrogenophosphonate ions depends entirely on the water content in the solution. Monolayers are favored with water contents that are less than 5%, whereas thicker layers are formed from solutions with a higher percentage of H_2O, indicating that water induces molecular aggregation. A question that remains open is whether the organic layer is formed on the gallium arsenide sites or on the oxidized sites. This study also shows that gallium sites are preferred, but no definite answer can be obtained concerning their oxidation state.

Acknowledgment. This work is part of the Growth project No. G5RD-CT-2001-00569 SENTIMATS financed by EU. We also acknowledge the "Financiamento Plurianual" from FCT (Portugal) and the project GRICES/ Ambassade Française in Portugal.

Appendix

The XPS atomic ratios for the main elements that are present on the surface are shown in Table 3.

LA050682+